

1 **Evidence of cryptic methane cycling and non-methanogenic**
2 **methylamine consumption in the sulfate-reducing zone of**
3 **sediment in the Santa Barbara Basin, California**

4 Sebastian J.E. Krause^{1*#}, Jiarui Liu¹, David J. Yousavich¹, DeMarcus Robinson², David W.
5 Hoyt³, Qianhui Qin⁴, Frank Wenzhoefer^{5,6,7}, Felix Janßen^{5,6}, David L. Valentine⁸, and Tina
6 Treude^{1,2*}

7 ¹Department of Earth Planetary and Space Sciences, University of California, Los Angeles, CA
8 90095, USA

9 ²Department of Atmospheric and Ocean Sciences, University of California, Los Angeles, CA
10 90095, USA

11 ³Pacific Northwest National Laboratory Environmental and Molecular Sciences Division,
12 Richland, WA 99352, USA

13 ⁴Interdepartmental Graduate Program in Marine Science, University of California, Santa
14 Barbara, CA 93106, USA

15 ⁵HGF-MPG Group for Deep-Sea Ecology and Technology, Alfred-Wegener-Institute,
16 Helmholtz-Center for Polar and Marine Research, Am Handelshafen 12, 27570 Bremerhaven,
17 Germany

18 ⁶Max Planck Institute for Marine Microbiology, Celsiusstrasse 1, 28359 Bremen, Germany

19 ⁷Department of Biology, DIAS, Nordcee and HADAL Centres, University of Southern
20 Denmark, 5230 Odense M, Denmark

21 ⁸Department of Earth Science and Marine Science Institute, University of California Santa
22 Barbara, Santa Barbara, CA 93106, USA

23 *Correspondence: Sebastian Krause (sjkrause@ucsb.edu), Tina Treude (ttreude@g.ucla.edu)

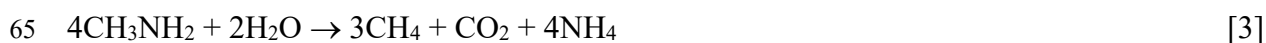
24 **# Present address: Earth Research Institute, 6832 Ellison Hall, University of California**
25 **Santa Barbara, Ca 93106-3060**

26 **Abstract.** The recently discovered cryptic methane cycle in the sulfate-reducing zone of marine
27 and wetland sediments couples methylotrophic methanogenesis to anaerobic oxidation of
28 methane (AOM). Here we present evidence of cryptic methane cycling activity within the
29 upper regions of the sulfate-reducing zone, along a depth transect within the Santa Barbara
30 Basin, off the coast of California, USA. The top 0-20 cm of sediment from each station was
31 subjected to geochemical analyses and radiotracer incubations using $^{35}\text{S-SO}_4^{2-}$, ^{14}C -mono-
32 methylamine, and $^{14}\text{C-CH}_4$ to find evidence of cryptic methane cycling. Methane
33 concentrations were consistently low (3 to 16 μM) across the depth transect, despite AOM rates
34 increasing with decreasing water depth (from max 0.05 $\text{nmol cm}^{-3} \text{d}^{-1}$ at the deepest station to
35 max 1.8 $\text{nmol cm}^{-3} \text{d}^{-1}$ at the shallowest station). Porewater sulfate concentrations remained
36 high (23mM to 29 mM), despite the detection of sulfate reduction activity from $^{35}\text{S-SO}_4^{2-}$
37 incubations with rates up to 134 $\text{nmol cm}^{-3} \text{d}^{-1}$. Metabolomic analysis showed that substrates
38 for methanogenesis (i.e., acetate, methanol and methylamines) were mostly below the detection
39 limit in the porewater, but some samples from the 1-2 cm depth section showed non-
40 quantifiable evidence of these substrates, indicating their rapid turnover. Estimated
41 methanogenesis from mono-methylamine ranged from 0.2 nmol to 0.5 $\text{nmol cm}^{-3} \text{d}^{-1}$.
42 Discrepancies between the rate constants (K_1) of methanogenesis (from ^{14}C - mono-
43 methylamine) and AOM (from either ^{14}C - mono-methylamine-derived $^{14}\text{C-CH}_4$ or from
44 directly injected $^{14}\text{C-CH}_4$) suggest the activity of a separate, concurrent metabolic process
45 directly metabolizing mono-methylamine to inorganic carbon. We conclude that the results
46 presented in this work show strong evidence of cryptic methane cycling occurring within the
47 top 20 cm of sediment in the Santa Barbara Basin. The rapid cycling of carbon between
48 methanogenesis and methanotrophy likely prevents major build-up of methane in the sulfate-
49 reducing zone. Furthermore, our data suggest that methylamine is utilized by both
50 methanogenic archaea capable of methylotrophic methanogenesis and non-methanogenic

51 microbial groups. We hypothesize that sulfate reduction is responsible for the additional
52 methylamine turnover but further investigation is needed to elucidate this metabolic activity.
53

54 **1. Introduction**

55 In anoxic marine sediment, methane is produced by microbial methanogenesis in the
56 last step of organic carbon remineralization (Stephenson and Stickland, 1933; Thauer, 1998;
57 Reeburgh, 2007). This methane is produced by groups of obligate anaerobic methanogenic
58 archaea across the Euryarchyota, Crenarchaeota, Halobacterota, and Thermoplasmata phyla
59 (Lyu et al., 2018). Methanogens can produce methane through three different metabolic
60 pathways, using CO₂ (CO₂ reduction; e.g., hydrogenotrophic) (Eq. 1), acetate (acetoclastic)
61 (Eq. 2) and methylated substrates such as, methyl sulfides, methanol, and methylamines
62 (methylotrophic) (e.g., Eq. 3).



66 Classically, hydrogenotrophic and acetoclastic methanogenesis are dominant in deeper
67 sulfate-free sediment (Jørgensen, 2000; Reeburgh, 2007). This distinct geochemical zonation
68 is due to the higher free energy gained by sulfate-reducing bacteria within the sulfate reduction
69 zone coupling sulfate reduction with hydrogen and/or acetate consumption in sulfate-rich
70 sediment. Thus, sulfate-reducing bacteria tend to outcompete methanogenic archaea for
71 hydrogen and acetate in shallower sediment layers in the presence of sulfate (Kristjansson et
72 al., 1982; Winfrey and Ward, 1983; Lovley and Klug, 1986; Jørgensen, 2000). However,
73 methylotrophic methanogenesis is known to occur within the sulfate-reducing zone. The
74 activity of this process in the presence of sulfate reduction is possible because methylated
75 substrates, such as methylamines, are non-competitive carbon sources for methanogens
76 (Oremland and Taylor, 1978; Lovley and Klug, 1986; Maltby et al., 2016; Zhuang et al., 2016;
77 2018; 2018; Krause and Treude, 2021). Methylotrophic methanogenesis activity in the sulfate-
78 reducing zone has been detected in a wide range of aquatic environments, such as coastal
79 wetlands (Oremland et al., 1982; Oremland and Polcin, 1982; Krause and Treude, 2021),

80 upwelling regions (Maltby et al., 2016), and eutrophic shelf sediment (Maltby et al., 2018; Xiao
81 et al., 2018). Despite methylotrophic activity in the sulfate-reducing zone, methane
82 concentrations are several orders of magnitude lower than methane concentrations found in
83 deeper sediment zones where sulfate concentrations are depleted (Barnes and Goldberg, 1976;
84 Dale et al., 2008b; Wehrmann et al., 2011; Beulig et al., 2018).

85 In anoxic marine sediment, anaerobic oxidation of methane (AOM) is an important
86 methane sink that is typically coupled to sulfate reduction (Eq. 4) and mediated by a consortium
87 of anaerobic methane-oxidizing archaea (ANME) and sulfate-reducing bacteria (Knittel and
88 Boetius, 2009; Orphan et al., 2001; Michaelis et al., 2002; Boetius et al., 2000; Hinrichs and
89 Boetius, 2002; Reeburgh, 2007).



91 AOM occurring in the sulfate-reducing zone, fuelled by concurrent methylotrophic
92 methanogenesis activity, i.e., the cryptic methane cycle, could be the reason why methane
93 concentrations are consistently low in sulfidic sediment (Krause and Treude, 2021; Xiao et al.,
94 2017; Xiao et al., 2018). These studies highlight the importance of the cryptic methane cycle
95 on the global methane budget. However, the extent of our knowledge of cryptic methane cycle
96 is restricted to a few aquatic environments. Thus, it is crucial to investigate and understand the
97 cryptic methane cycle in other aquatic environments to fully understand its impact on the global
98 methane budget. In the present study we focus on organic-rich sediment below oxygen-
99 deficient water in the Santa Barbara Basin (SSB), California.

100 Oxygen minimum zones (OMZ) are regions where high oxygen demand in the water
101 column leads to a dramatic decline or even absence of dissolved oxygen (Wright et al., 2012;
102 Paulmier and Ruiz-Pino, 2009; Wyrski, 1962; Canfield and Kraft, 2022). In these
103 environments, coastal upwelling of nutrients results in high phytoplankton growth, greatly
104 enhancing organic matter loading and in turn creating a high metabolic oxygen demand during
105 organic matter degradation in the water column. This enhanced respiration depletes oxygen

106 faster than it is replenished (especially in poorly ventilated water bodies), which results in
107 seasonal or continuous low oxygen conditions (Wyrski, 1962; Helly and Levin, 2004; Wright
108 et al., 2012; Levin et al., 2009). Sediment beneath OMZs is typically rich in organic matter
109 supporting predominantly or exclusively anaerobic degradation processes, including
110 methanogenesis (Levin, 2003; Rullkötter, 2006; Middelburg and Levin, 2009; Fernandes et al.,
111 2022; Treude, 2011). Thus, sediments underlying OMZ's are good candidate environments to
112 investigate cryptic methane cycling.

113 Located within the Pacific Ocean, between the Channel Islands and the mainland of
114 Santa Barbara, California, USA, the SBB is characterized as a thermally stratified, coastal
115 marine basin with a maximum water column depth of approximately 590 m (Soutar and Crill,
116 1977; Arndt et al., 1990; Sholkovitz, 1973). Low oxygen concentrations (<10 μM) are found
117 in the bottom waters below the sill depth (~475 m) of the SBB (Sholkovitz, 1973; Reimers et
118 al., 1996). The sediment in the SBB have an organic carbon content between 2-6%
119 (Schimmelmann and Kastner, 1993). These characteristics make the SBB a prime study site to
120 find evidence of cryptic methane cycling.

121 Organic carbon sources for methylotrophic methanogenesis, such as methylamine, are
122 ubiquitous in coastal marine environments (Zhuang et al., 2018; Zhuang et al., 2016; Oren,
123 1990), including marine environments where OMZ's exist (Ferdelman et al., 1997; Gibb et al.,
124 1999). Methylamines are derived from osmolytes, such as glycine and betaine, and are
125 synthesized by phytoplankton (Oren, 1990). However, the abundance of methylamines and
126 how they may be driving cryptic methane cycling in anoxic sediment within OMZ's is virtually
127 unknown. Furthermore, the fate of methane from methylotrophic methanogenesis in the sulfate
128 reduction zone is poorly constrained. Particularly, if cryptic methane cycling is active above
129 the sulfate-methane transition zone, gross production and consumption of methane have likely
130 been underestimated. Therefore, finding evidence for the cryptic methane cycle in the SBB is

131 a necessary step towards understanding how carbon is cycled through the sediment of the SBB
132 and other OMZs.

133 In the present study we report biogeochemical evidence of cryptic methane cycling in
134 surface sediment (top ~15 cm) collected along a depth transect crossing the SBB. We applied
135 the radiotracer method from Krause and Treude (2021) to trace the production of methane from
136 mono-methylamine, followed by the anaerobic oxidation of methane to inorganic carbon. We
137 combined this approach with standard radiotracer methods for the detection of AOM and
138 sulfate reduction as well as with analyses of sediment porewater geochemistry.
139

140 **2. Methods.**

141 **2.1. Study site and sediment sampling**

142 Sediment samples were collected during the R/V *Atlantis* expedition AT42-19 in fall
143 2019. Collection was achieved with polycarbonate push cores (30.5 cm long, 6.35 cm i.d.),
144 which were deployed by the ROV *JASON* along a depth transect through the SBB. The depth
145 transect selected for this particular study, was the Northern Deposition Transect 3 (NDT3),
146 with three stations (NDT3-A, -C and -D), as well as the Northern Depositional Radial Origin
147 (NDRO), and the Southern Depositional Radial Origin (SDRO) station, located in the deepest
148 part of the basin. Details on the stations' water column depths and near-seafloor oxygen
149 concentrations are provided in Table 1.

150 **Table 1.** Water column depth, bottom water oxygen concentrations and coordinates of each station sampled during
151 this study.

Station	Depth (m)	Bottom Water Oxygen (μM)	Latitude	Longitude
SDRO	586	0	34.2011	-120.0446
NDRO	580	0	34.2618	-120.0309
NDT3-A	572	9.2	34.2921	-120.0258
NDT3-C	498	5	34.3526	-120.0160
NDT3-D	447	8	34.3625	-120.0150

152
153 After sediment collection, ROV push cores were returned to the surface by an elevator
154 platform. Upon retrieval onboard the R/V *Atlantis*, sediment samples were immediately
155 transported to an onboard cold room (6°C) for further processing of biogeochemical parameters
156 (see details in section 2.2.).

157

158 **2.2. Sediment porewater sampling and sulfate analysis**

159 For porewater analyses, two ROV sediment push cores from each station were sliced
160 in 1-cm increments in the top 10 cm of the sediment, followed by 2-cm increments below.

161 During sediment sampling, ultra-pure argon was flushed over the sediment to minimize
162 oxidation of oxygen sensitive species. The sliced sediment layers were quickly transferred to
163 argon-flushed 50 mL plastic centrifuge vials and centrifuged at 2300 X g for 20 mins to extract
164 the porewater. Subsequently, 2 mL of porewater was subsampled from the supernatant and
165 frozen at -20 °C for shore-based sulfate analysis by ion chromatography (Metrohm 761)
166 following (Dale et al., 2015). Additional porewater (1 mL) was subsampled for the
167 determination of the concentration of methylamine and other metabolic substrates (see section
168 2.4).

169

170 ***2.3. Sediment methane and benthic methane flux analyses***

171 Methane concentration in the sediment was determined from a replicate ROV pushcore.
172 Sediment was sliced at 1-cm increments in the top 10 cm, followed by 2-cm increments below.
173 Two mL of sediment was sampled with a cut-off 3 mL plastic syringe and quickly transferred
174 to 12 mL glass serum vials filled with 5 mL 5% (w/w) NaOH solution. The vials were sealed
175 immediately with a grey butyl rubber stopper and aluminum crimps, shaken thoroughly, and
176 stored upside down at 4 °C. Methane concentrations in the headspace were determined shore-
177 based using a gas chromatograph (Shimadzu GC-2015) equipped with a packed Haysep-D
178 column and flame ionization detector. The column was filled with helium as a carrier gas,
179 flowing at 12 mL per minute and heated to 80 °C. Methane concentrations in the environmental
180 samples were calibrated against methane standards (Scott Specialty Gases) with a \pm 5%
181 precision.

182 To determine methane flux out of the sediment and into the water column, 1-2
183 custom-built cylindrical benthic flux chambers (BFC) (Treude et al., 2009) were deployed at
184 each sampling station by the ROV Jason. The BFCs consist of a lightweight fiber-reinforced
185 plastic frame, which holds a cylindrical polycarbonate chamber. Buoyant syntactic foam was
186 attached to the feet of the frame to keep the BFC's from sinking too deep into the soft and

187 poorly consolidated sediments, especially in the deeper stations. Water overlying the
188 enclosed sediment was kept mixed with a stirrer bar rotating below the lid of the chamber.
189 The BFC's were equipped with a syringe sampler holding seven, 50 mL glass syringes (6
190 syringes for sample collection and 1 syringe for freshwater injection). One sample syringe
191 withdrew 50 mL of seawater from the chamber volume at pre-programed time intervals. The
192 seventh syringe was used to inject 50 mL of de-ionized water into the chamber shortly after
193 deployment to calculate the volume from the change in salinity in the overlying seawater
194 recorded by a conductivity sensor (type 5860, Aanderaa Data Instruments, Bergen, NO),
195 according to (Kononets et al., 2021).

196 Seawater samples to determine the methane flux out of the sediments were collected
197 in 26 mL serum glass bottles. The 26 mL serum bottles were acid cleaned, and then
198 combusted at 300 °C prior to BFC seawater sample collection. One to two pellets of solid
199 NaOH were added into each empty 26 mL combusted serum bottle. All empty serum bottles
200 were then flushed with ultra-pure nitrogen gas (Airgas Ultra High Purity Grade Nitrogen,
201 Manufacturer Part #:UHP300) for 5 min, then sealed with autoclaved chlorobutyl stoppers
202 and crimps. Lastly, a vacuum pump was used to evacuate the bottles to a pressure down to
203 <0.05 psi prior to sample collection.

204 Immediately after BFC recovery from the seafloor, approximately 20 mL of seawater
205 sample was transferred into the pre-evacuated, acid cleaned, and combusted 26 mL glass
206 serum bottles through the chlorobutyl stopper using a sterile 23G needle. Pressure within the
207 serum bottle was equalized to atmospheric pressure with the introduction of UHP grade
208 nitrogen. Serum bottles were shaken to dilute the NaOH pellets, which terminated metabolic
209 activity and forced the dissolved methane into the gas headspace. The serum bottles were
210 reweighed after sample collection, to calculate the exact volume of the seawater sample.
211 Methane concentrations in seawater collected from the BFC's were analyzed shipboard by
212 gas chromatography according to Qin et al., 2022.

213 Total methane concentration in the headspace was calculated following the ideal gas
214 law Eq. (5),

$$215 \quad n = \frac{PV}{RT} * [CH_4] * \frac{1}{V_{SW}} . \quad [5]$$

216 Where n is the total molar concentration of methane, P is atmospheric pressure, V is the volume
217 of the headspace of serum bottle (which is calculated by 26 mL subtracted by the volume of
218 seawater sample), R is the ideal gas constant, T is temperature in Kelvin (288.15 K), $[CH_4]$ is
219 the methane measured by GC as percentage values in ppm, and V_{SW} is the volume of seawater
220 in the serum vial. The volume of sampled seawater in each serum bottle was calculated by
221 subtracting the mass of the empty serum bottle from the mass of the filled serum bottle,
222 normalized by the density of seawater.

223

224 ***2.4. Determination of methanogenic substrates in porewater***

225 To obtain sediment porewater concentrations of methanogenic substrates
226 (methylamine, methanol, and acetate), 1 mL porewater was extracted from 1-2 cm and 9-10
227 cm depth sections at each station (see section 2.2) and syringe-filtered (0.2 μ m) into pre-
228 combusted (350 °C for 3 hrs) amber glass vials (1.8 mL), which were then closed with a PTFE
229 septa-equipped screw caps and frozen at -80 °C until analyses. Samples were analysed at the
230 Pacific Northwest National Laboratory, Environment and Molecular Sciences Division for
231 metabolomic analysis using proton nuclear magnetic resonance (NMR). Prior to analysis,
232 porewater samples were diluted by 10% (v/v) with an internal standard (5 mM 2,2-dimethyl-
233 2-silapentane-5-sulfonate-d6). All NMR spectra were collected using an 800 MHz Bruker
234 Avance Neo (Tava), with a TCI 800/54 H&F/C/N-D-05 Z XT, and an QCI H-P/C/N-D-05 Z
235 ET extended temperature range CryoProbe. The 1D 1H NMR spectra of all samples were
236 processed, assigned, and analysed by using the Chenomx NMR Suite 8.6 software with
237 quantification based on spectral intensities relative to the internal standard. Candidate
238 metabolites present in each of the complex mixture were determined by matching the chemical

239 shift, J-coupling, and intensity information of experimental NMR signals against the NMR
240 signals of standard metabolites in the Chenomx library. The 1D ^1H spectra were collected
241 following standard Chenomx data collection guidelines, employing a 1D NOESY presaturation
242 experiment (noesypr1d) with 65536 complex points and at least 4096 scans at 298 K. Signal to
243 noise ratios (S/N) were measured using MestReNova 14 with the limit of quantification equal
244 to a S/N of 10 and the limit of detection equal to a S/N of 3. The 90° ^1H pulse was calibrated
245 prior to the measurement of each sample with a spectral width of 12 ppm and 1024 transients.
246 The NOESY mixing time was 100 ms and the acquisition time was 4 s followed by a relaxation
247 delay of 1.5 s during which presaturation of the water signal was applied. Time domain free
248 induction decays (72114 total points) were zero-filled to 131072 total points prior to Fourier
249 transform.

250

251 ***2.5. Metabolic activity determinations***

252 One replicate ROV sediment push core (hereafter 'ROV rate push core') from each
253 station was sub-sampled with three mini-cores (20 cm long, 2.6 cm i.d.) for radiotracer
254 incubations according to the whole-core injection method (Jørgensen 1978) to collect
255 quantitative metabolic evidence (sulfate reduction, methanogenesis, methane oxidation) of
256 cryptic methane cycling. The incubation methods are detailed below. Note that not enough
257 sediment cores were collected at each station to perform replicate radiotracer experiments that
258 would have allowed addressing small-scale spatial variability in ex-situ rates.

259

260 ***2.5.1. Sulfate reduction via ^{35}S -Sulfate***

261 Within the same day of collection, one mini-core from each ROV rate push core was
262 used to determine sulfate-reduction rates. Radioactive carrier-free ^{35}S -sulfate ($^{35}\text{S}\text{-SO}_4^{2-}$;
263 dissolved in MilliQ water, injection volume 10 μL , activity 260 KBq, specific activity 1.59
264 TBq mg^{-1}) was injected into the mini core at 1-cm increments and incubated at 6 $^\circ\text{C}$ in the dark

265 following (Jørgensen, 1978). Injected sediment cores were stored vertically and incubated for
266 ~6 hrs at 6 °C in the dark. Incubations were stopped by slicing the sediment in 1-cm increments
267 into 50 mL plastic centrifuge tubes containing 20 mL 20% (w/w) zinc acetate solution. Each
268 sediment sample was sealed and shaken thoroughly and stored at -20 °C to halt metabolic
269 activity. For the control samples, sediments were added to zinc acetate solution prior to
270 radiotracer injection. In the home laboratory, sulfate reduction rates were determined using the
271 cold-chromium distillation method (Kallmeyer et al., (2004).

272

273 ***2.5.2. Methanogenesis and AOM via ¹⁴C-Mono-Methylamine***

274 This study aimed at determining the activity of methanogenesis from mono-
275 methylamine (MG-MMA) and the subsequent anaerobic oxidation of the resulting methane to
276 inorganic carbon by AOM (AOM-MMA). To accomplish this goal, a mini core from each ROV
277 rate push core was injected with radiolabeled ¹⁴C-mono-methylamine (¹⁴C-MMA; dissolved in
278 1 mL water, injection volume 10 µL, activity 220 KBq, specific activity 1.85-2.22 GBq mmol⁻¹)
279 similar to section 2.5.1. After 24 hrs, the incubation was terminated by slicing the sediment
280 at 1-cm increments into 50 mL wide mouth glass vials filled with 20 mL of 5% NaOH. Five
281 killed control samples were prepared by transferring approximately 5 ml of extra sediment
282 from each station into 50 mL wide mouth vials filled with 20 mL of 5% NaOH prior to
283 radiotracer addition. Sample vials and vials with killed controls were immediately sealed with
284 butyl rubber stoppers and aluminium crimps and shaken thoroughly for 1 min to ensure
285 complete biological inactivity. Vials were stored upside down at room temperature until further
286 processing. In the home laboratory, methane production from ¹⁴C-MMA by MG-MMA and
287 subsequent oxidation of the produced ¹⁴C-methane (¹⁴C-CH₄) by AOM-MMA was determined
288 according to the adapted radiotracer method outlined in (Krause and Treude, 2021).

289 To account for ^{14}C -MMA potentially bound to mineral surfaces (Wang and Lee, 1993,
 290 1994; Xiao et al., 2022), we determined the ^{14}C -MMA recovery factor (RF) for the sediment
 291 from the stations NDT3-C, D and NDRO according to Krause and Treude (2021).

292 Metabolic rates of MG-MMA were calculated according to Eq. 7. Note that natural
 293 concentrations of MMA in the SBB sediment porewater were either below detection or
 294 detectable, but below the quantification limit ($<10\ \mu\text{M}$) (Table S1). Therefore, MMA
 295 concentrations were assumed to be $3\ \mu\text{M}$ to calculate the ex-situ rate of MG-MMA (Eq. 8).

$$296 \quad MG-MMA = \frac{a_{CH_4} + a_{TIC}}{a_{CH_4} + a_{TIC} + \left[\frac{a_{MMA}}{RF}\right]} * [MMA] * \frac{1}{t} \quad [7]$$

297 where *MG-MMA* is the rate of methanogenesis from mono-methylamine ($\text{nmol cm}^{-3} \text{d}^{-1}$); a_{CH_4}
 298 is the radioactive methane produced from methanogenesis (CPM); a_{TIC} is the radioactive total
 299 inorganic carbon produced from the oxidation of methane (CPM); a_{MMA} the residual
 300 radioactive mono-methylamine (CPM); RF is the recovery factor (Krause and Treude, (2021)
 301 ; $[MMA]$ is the assumed mono-methylamine concentrations in the sediment (nmol cm^{-3}); t is
 302 the incubation time (d). ^{14}C - CH_4 and ^{14}C -TIC sample activity was corrected by respective
 303 abiotic activity determined in killed controls.

304 Results from the ^{14}C -MMA incubations were also used to estimate the AOM-MMA
 305 rates according to Eq. 8,

$$306 \quad AOM-MMA = \frac{a_{TIC}}{a_{CH_4} + a_{TIC}} * [CH_4] * \frac{1}{t} \quad [8]$$

307 where *AOM-MMA* is the rate of anaerobic oxidation of methane based on methane produced
 308 from MMA ($\text{nmol cm}^{-3} \text{d}^{-1}$); a_{TIC} is the produced radioactive total inorganic carbon (CPM); a_{CH_4}
 309 is the residual radioactive methane (CPM); $[CH_4]$ is the sediment methane concentration (nmol
 310 cm^{-3}); t is the incubation time (d). ^{14}C -TIC activity was corrected by abiotic activity determined
 311 by replicate dead controls.

312

313 **2.5.3 Anaerobic oxidation of methane via ^{14}C -Methane**

314 AOM rates from $^{14}\text{C-CH}_4$ (AOM- CH_4) were determined by injecting radiolabeled $^{14}\text{C-}$
315 CH_4 (dissolved in anoxic MilliQ, injection volume 10 μL , activity 5 KBq, specific activity
316 1.85–2.22 GBq mmol^{-1}) into one mini core from each ROV rate core at 1-cm increments similar
317 to section 2.5.1. Incubations of the mini cores were stopped after ~24 hours similar to section
318 2.5.2. In the laboratory, AOM- CH_4 was analysed using oven combustion (Treude et al., 2005)
319 and acidification/shaking (Joye et al., 2004). The radioactivity was determined by liquid
320 scintillation counting. AOM- CH_4 rates were calculated according to Eq. 8.

321

322 ***2.5.4 Rate constants for AOM- CH_4 , MG-MMA, and AOM-MMA***

323

324 Metabolic rate constants (k) for AOM- CH_4 , MG-MMA and AOM-MMA were calculated for
325 relative turnover comparisons using the experimental data determined by sections 2.5.2 and
326 2.5.3. The rate constants consider the metabolic reaction products, divided by the sum of
327 reaction reactants and products and by time. The metabolic rate constants for AOM- CH_4 , MG-
328 MMA and AOM-MMA were calculated according to Eq. 9,

$$329 \quad k = \frac{a_{products}}{a_{products} + a_{reactants}} * \frac{1}{t} \quad [9]$$

330 where k is the metabolic rate constant (day^{-1}); $a_{products}$ is the radioactivity (CPM) of the
331 metabolic reaction products; $a_{reactants}$ is the radioactivity (CPM) of the metabolic reaction
332 reactants; t is time in days.

333

334 **3. Results**

335 **3.1. Sediment biogeochemistry**

336 At most stations, porewater methane concentrations in the top 10-20 cm of sediment
337 fluctuated between 3 and 13 μM with no clear trend (Fig. 1A, E, I, M, and Q). At NDRO,
338 methane steadily increased below 12 cm, reaching 16 μM at 14–15 cm (Fig. 1E). Methane
339 concentrations determined in water samples from the BFC incubations revealed only minor
340 fluctuations over time with no clear trends, suggesting no net fluxes of methane into or out of
341 the sediment at all stations (Fig. 1S). It is notable, however, that the BFCs captured higher
342 methane concentrations (350-800 nM) in the supernatant of station SDRO, NDRO, and NDT3-
343 A compared to NDT3-C and NDT3-D (< 130 nM). Sulfate concentrations showed no strong
344 decline with depth at any station (except maybe a weak tendency at SDRO and NDT3-A) and
345 fluctuated between 23 and 30 mM in the sampled top 10-20 cm (Fig. 1A, E, I, M, and Q).

346 Table S1 provides porewater concentrations of organic carbon sources from the
347 metabolomic analysis, as measured by NMR, that are known to support methanogenesis.
348 Methylamine was detected at SDRO and NDT3-A (1–2 cm), but those concentrations were
349 below the quantification limit (10 μM). Otherwise, methylamine was below detection (<3 μM)
350 for all other samples. Similarly, methanol was detected but below quantification at NDT3-A
351 (1–2 cm) but otherwise below detection. Acetate was at a quantifiable level (21 μM) at NDT3-
352 A (1–2 cm) but was otherwise either below quantification (SDRO, 1-2 cm; NDRO, 1-2 cm) or
353 below detection.

354

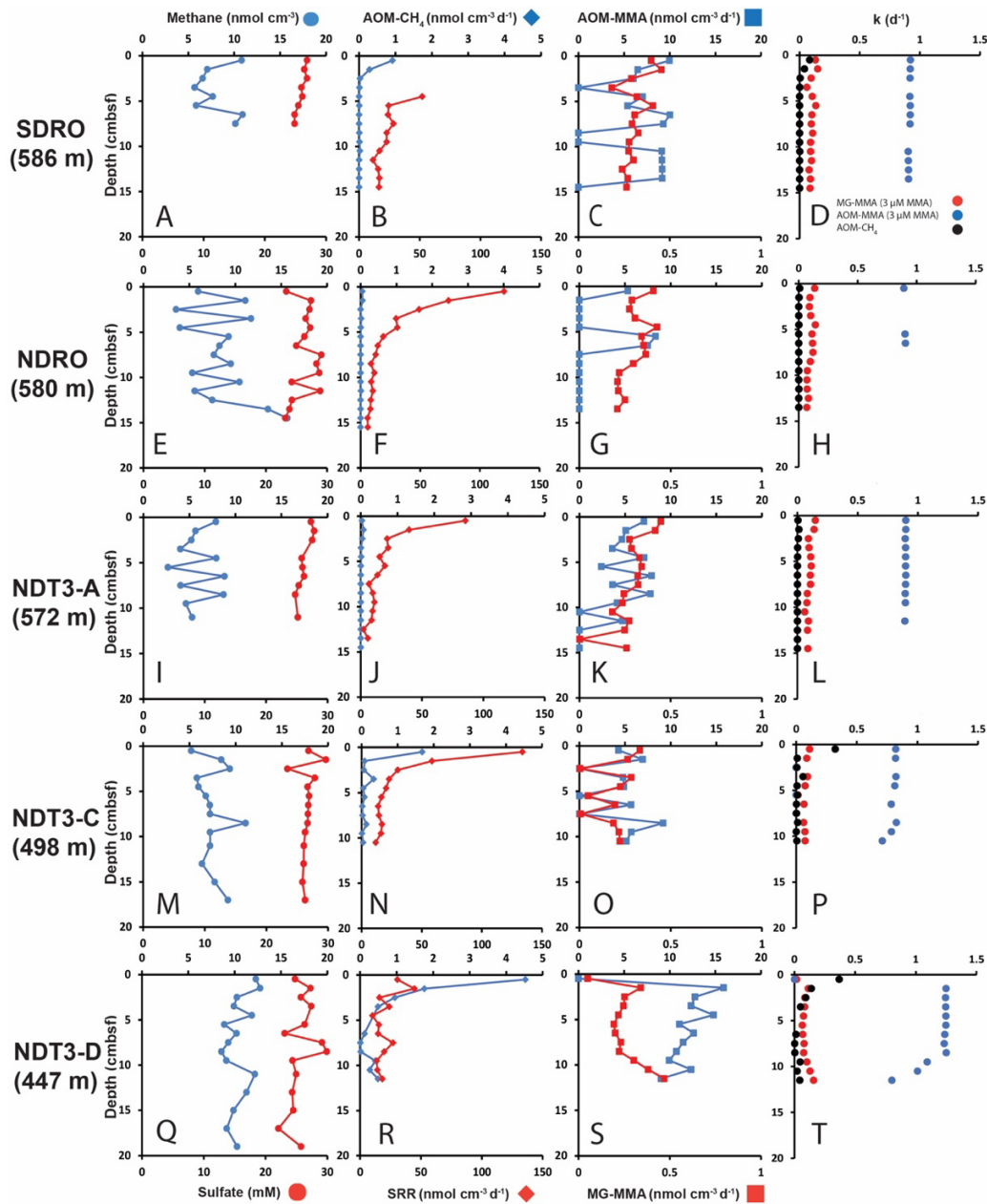
355 **3.2 AOM from ^{14}C -methane and sulfate reduction from ^{35}S -sulfate**

356 Fig. 1B, F, J, N, and R depict ex-situ rates of AOM- CH_4 and sulfate reduction from the
357 radiotracer incubations with ^{14}C -methane and ^{35}S -sulfate in sediment mini cores, respectively.
358 AOM- CH_4 activity tended to increase with decreasing water depth in the top 5 cm of the
359 sediment (from max 0.05 $\text{nmol cm}^{-3} \text{d}^{-1}$ at NDRO to max 4.5 $\text{nmol cm}^{-3} \text{d}^{-1}$ at NDT3-D), while

360 rates were either negligible (SDRO, NDRO, NDT3-A) or $<1 \text{ nmol cm}^{-3} \text{ d}^{-1}$ (NDT3-C, NDT3-
361 D) for depths $>5 \text{ cm}$. Where peaks in AOM were present (SDRO, NDT3-C, NDT3-D) they
362 were always located in the top 0–1 cm sediment layer.

363 Sulfate reduction activity was detected throughout all sediment cores with the highest
364 rates mostly at 0–1 cm, followed by a decrease with increasing sediment depth. The highest
365 individual sulfate reduction peaks were found at NDRO, NDT3-A, and NDT3-C (120, 85 and
366 $133 \text{ nmol cm}^{-3} \text{ d}^{-1}$). At NDT3-D sulfate reduction rates varied between 14 and $45 \text{ nmol cm}^{-3} \text{ d}^{-1}$
367 throughout the core with no clear trend. Note that sulfate reduction data are missing for 0–5
368 cm at SDRO, due to post-cruise analytical issues. Here, rates gradually decreased from 52 to
369 $10 \text{ nmol cm}^{-3} \text{ d}^{-1}$ below 5 cm.

370



371

372 **Figure 1.** Depth profiles of biogeochemical parameters in sediment across the depth transect of the Santa Barbara
 373 Basin. A, E, I, M, and Q: sediment methane and porewater sulfate; B, F, J, N, and R: AOM-CH₄ and sulfate
 374 reduction (determined from direct injection of ¹⁴C-CH₄ and ³⁵S-Sulfate, respectively); C, G, K, O, and S:
 375 MMA and MG-MMA (determined from direct injection of ¹⁴C-MMA); D, H, L, P, and T: rate constants for AOM-
 376 CH₄, MG-MMA and AOM-MMA.

377 **3.3 Methanogenesis and AOM from ^{14}C -mono-methylamine**

378 **3.3.1 ^{14}C -MMA recovery from sediment**

379 RF values determined in sediments from NDRO, NDT3-C and D stations (see section
380 2.5.2) were 0.93, 0.84, and 0.75, respectively. They were used to correct MG-MMA rates at
381 each station of the study. Note that no RF values were determined for SDRO or the NDT3-A.
382 We applied RF values from NDRO and NDT3-C, respectively, instead.

383

384 **3.3.2 MG-MMA and AOM-MMA**

385 Fig. 1C, G, K, O, S show ex-situ rates of MG-MMA and AOM-MMA, assuming a
386 natural MMA concentration of 3 μM (see section 2.5.2). At SDRO, NDRO, and NDT3-A, MG-
387 MMA ranged between 0.27 and 0.45 $\text{nmol cm}^{-3} \text{d}^{-1}$ throughout the sediment core without trend
388 (Fig. 1C, G, and K). At NDT3-C MG-MMA ex-situ rates were lower ranging between 0.007
389 $\text{nmol cm}^{-3} \text{d}^{-1}$ and 0.3 $\text{nmol cm}^{-3} \text{d}^{-1}$ without any pattern (Fig. 1O). At NDT3-D, MG-MMA
390 sharply increased from 0.05 $\text{nmol cm}^{-3} \text{d}^{-1}$ at 0–1cm, to $\sim 0.34 \text{ nmol cm}^{-3} \text{d}^{-1}$ at 1–2 cm. MG-
391 MMA then decreased slightly to $\sim 0.2 \text{ nmol cm}^{-3} \text{d}^{-1}$ between 2 and 9 cm, before increasing to
392 $\sim 0.5 \text{ nmol cm}^{-3} \text{d}^{-1}$ at the bottom of the core (Fig. 1S).

393 AOM-MMA rates were 1 to 2 orders of magnitude higher than MG-MMA rates and 1
394 to 4 orders of magnitude higher than AOM- CH_4 rates (Fig 1C, G, K, O, S). At SDRO, NDRO,
395 NDT3-A, and NDT3-C, AOM-MMA ex-situ rates ranged between 5.3 and 10 $\text{nmol cm}^{-3} \text{d}^{-1}$
396 (unless zero) with no trend (Fig 1C, G, K, and O). At NDT3-D, AOM-MMA rates decreased
397 from 15.9 $\text{nmol cm}^{-3} \text{d}^{-1}$ at 1–2 cm to 9 $\text{nmol cm}^{-3} \text{d}^{-1}$ at 11–12 cm (Fig. 1S). At all stations,
398 some sediment intervals showed no biological net AOM-MMA activity (Fig 1C, G, K, O, S).
399 In these sediment intervals, the ^{14}C -TIC activity was statistically not different from the average
400 plus the standard deviation of the killed control samples.

401

402 **3.4 Rate constants for MG-MMA, AOM-MMA and AOM- CH_4**

403 Fig. 1D, H, L, P, and T show the rate constants (k) for MG-MMA, AOM-MMA and
404 AOM-CH₄ for the comparison of relative radiotracer turnover. At all stations, MG-MMA rate
405 constants were between 0.01 and 0.15 d⁻¹. AOM-CH₄ rate constants ranged between 0.0009 d⁻¹
406 and 0.3 d⁻¹. Rate constants for AOM-MMA, however, were considerably higher than MG-
407 MMA and AOM-CH₄ with values ranging between 0.7 and 1.2 d⁻¹. Most rate constants
408 remained constant over depth, with the exemption of AOM-MMA at station NDT3-C and D
409 (Fig. 1P and T), which showed a steady decrease below 9 cm.

410 **4. Discussion**

411

412 **4.1. Evidence of cryptic methane cycling**

413 The aim of the present study was to check for the existence of cryptic methane cycling
414 in SBB surface sediments by presenting evidence for the concurrent activity of sulfate
415 reduction, AOM, and methanogenesis through radiotracer incubations (^{35}S - SO_4^{2-} , ^{14}C - CH_4 ,
416 and ^{14}C -MMA, respectively). Our study confirmed indeed that the three processes co-exist at
417 all investigated stations (Fig. 1). The most prominent concurrent metabolic activity was evident
418 from activity peaks near the sediment-water interface at station NDT3-C (Fig. 1N and O). We
419 suggest the concurrent peaking was stimulated by the availability of fresh, i.e., recently
420 deposited, organic matter coinciding with low oxygen concentrations in the bottom water
421 (Table 1). Fresh organic material likely provided a source for both organoclastic sulfate
422 reduction and methylotrophic methanogenesis, and indirectly (i.e., linked to the methane
423 produced) for AOM coupled to either nitrate, iron, or sulfate reduction. Low oxygen
424 concentrations offered favourable conditions for anaerobic processes in the surface sediment.
425 At the remaining stations (SDRO, NDRO, SDT3-A, SDT3-D; Fig. 1), metabolic activity of all
426 three processes was also confirmed near the sediment surface (with the exemption of the
427 missing data for sulfate reduction at SDRO), but they not always depicted rate peaks
428 (particularly not for AOM- CH_4).

429 Methane detected in the sulfate-rich sediment (Fig. 1A, E, I, M, Q) was likely produced
430 by methylotrophic methanogenesis utilizing non-competitive substrates within the sulfate-
431 reducing zone (Oremland and Taylor, 1978; King et al., 1983; Maltby et al., 2016; Maltby et
432 al., 2018; Reeburgh, 2007), which is also indicated by the production of methane from our ^{14}C -
433 MMA incubations. It is interesting to note that methane concentrations remained relatively
434 constant around 5 to 12 μM while AOM- CH_4 tended to increase with decreasing water depth.
435 This pattern suggests that the partial pressure of methane was likely determined by

436 thermodynamic equilibrium between methanogenesis and AOM (compare, e.g., with Conrad
437 1999).

438 The finding of non-linear methane concentrations in surface sediments is against the
439 general view that methane concentrations above the sulfate-methane transition zone show a
440 linear, diffusion-controlled decline towards the sediment-water interface, where methane
441 escapes into the water column (Reeburgh, 2007). We argue that the non-linear methane trends
442 we observe in the present study is an indication for simultaneous methane production and
443 consumption, i.e., cryptic methane cycling, as evident from our radiotracer experiments.

444 As there is considerable methanogenic activity even at the sediment-water interface (0-
445 1 cm) at all stations, aside from station NDT3-D (Fig. 1C, G, K, O, S), it is conceivable that
446 some methane could diffuse into the water column where it may be oxidized by either aerobic
447 or anaerobic oxidation processes (depending on the presence or absence of oxygen,
448 respectively) before emission into the atmosphere (Reeburgh, 2007). However, benthic
449 chamber incubations at the SBB stations did not indicate a release of methane into the water
450 column (Fig. S1), emphasizing the importance of cryptic methane cycling for preventing the
451 build-up of methane in the surface sediment and its emission into the water column.

452

453 ***4.2. Rapid turnover of metabolic substrates***

454 Natural porewater MMA concentrations were mostly below detection (<3 μM);
455 however, in porewater close to the sediment-water interface of SDRO and NDT3-A, MMA
456 was detected but below the quantification limit (<10 μM) (Table S1). Although we are unable
457 to report definitive MMA concentrations, we can bracket the MMA concentrations in a range
458 between 3 and 10 μM . The bracketed MMA concentrations are about 1 to 2 orders of magnitude
459 higher than what has been reported from porewater at other locations. For example, studies of
460 sediment porewater off the coast of Peru found MMA concentrations to be $\sim 0.15 \mu\text{M}$ (Wang
461 and Lee, 1990). Similarly, in sediment porewater collected from Buzzards Bay, Massachusetts

462 and in the Eastern Tropical North Pacific Ocean, MMA concentrations were either present at
463 trace amounts or below detection limit ($<0.05 \mu\text{M}$) (Lee and Olson, 1984). Detectable but low
464 methylamine concentrations in the porewater found in our study could imply that methylamines
465 are rapidly consumed by microbiological processes and/or removed from the porewater
466 through binding to minerals (Wang and Lee, 1990; Wang and Lee, 1993; Xiao et al., 2022).
467 Our study provided support for both hypotheses as we detected the biological potential for
468 MMA consumption via radiotracer (^{14}C -MMA) experiments (Fig. 1) and detected the binding
469 of 7-25% the injected ^{14}C -MMA to sediment (see 3.3.1).

470 Porewater methanol concentrations in the present study were also mainly below
471 detection, except for one sample, where it was not quantifiable (NDT3-A, 1–2 cm; Table S1).
472 In the marine environment, methanol is known to be a non-competitive substrate for
473 methanogenesis (King et al., 1983; Oremland and Taylor, 1978). However, a recent study
474 demonstrated that methanol is a carbon source for a wide variety of metabolisms, including
475 sulfate-reducing and denitrifying bacteria, as well as aerobic and anaerobic methylotrophs
476 (Fischer et al., 2021), which could all be present in the SBB sediments keeping methanol
477 concentrations low. Acetate was also detected in the metabolomic analysis but mostly below
478 quantification (except NDT3-A, 1–2 cm; Table S1). Acetate is formed through fermentation
479 reactions or through homoacetogenesis (Jørgensen, 2000; Ragsdale and Pierce, 2008). It is a
480 favourable food source for many bacteria and archaea such as sulfate reducers and
481 methanogens (Jørgensen, 2000; Conrad, 2020), which would explain its low concentration in
482 the SBB sediments. Low concentrations of the abovementioned metabolites are likely
483 signatures of rapid metabolic turnover, similar to what has been described for microbial
484 utilization of hydrogen in sediment (Conrad, 1999; Hoehler et al., 2001). In this situation,
485 metabolites would be kept at a steady-state concentration close to the thermodynamic
486 equilibrium of the respective consumers.

487

488 *4.3. Competitive methylamine turnover by non-methanogenic pathways*

489 Large disparities were found between AOM rates determined from the direct injection
490 of $^{14}\text{C-CH}_4$ (i.e., AOM- CH_4) and AOM determined from the production of $^{14}\text{C-TIC}$ in the $^{14}\text{C-}$
491 MMA incubations (i.e., AOM-MMA). AOM- CH_4 was roughly 1-2 orders of magnitude lower
492 compared to AOM-MMA (compare Fig. 1 B/C, F/G, J/K, N/O, R/S), indicating that AOM rates
493 determined via $^{14}\text{C-MMA}$ incubations were overestimated. We hypothesize that this disparity
494 is the result of the direct conversion of $^{14}\text{C-MMA}$ to $^{14}\text{C-TIC}$ by processes other than AOM
495 coupled to MG-MMA. Any process converting $^{14}\text{C-MMA}$ directly to $^{14}\text{C-TIC}$ would inflate
496 the rate constant only slightly for MG-MMA, but dramatically for AOM-MMA (see Eq. 8, 9,
497 and 10). Fig. 1D, H, L, P, and T confirm that the rate constants for AOM-MMA are 1 to 2
498 orders of magnitude higher compared to AOM- CH_4 and MG-MMA. We interpret the
499 difference in these rate constants to strongly suggests that the $^{14}\text{C-TIC}$ detected in the analysis
500 of samples incubated with $^{14}\text{C-MMA}$ must result not only from AOM involved in the cryptic
501 methane cycle but also from direct methylamine oxidation by a different anaerobic
502 methylotrophic metabolism that could not be disambiguated using the adapted radiotracer
503 method.

504 Methylamines are the simplest alkylated amine. They are derived from the degradation
505 of choline and betaine found in plant and phytoplankton biomass (Oren, 1990; Taubert et al.,
506 2017). The molecules are ubiquitously found in saline and hypersaline conditions in the marine
507 environment (Zhuang et al., 2016; Zhuang et al., 2017; Mausz and Chen, 2019). The
508 importance of methylamine as a nitrogen and carbon source for microbes to build biomass has
509 been well documented (Taubert et al., 2017; Capone et al., 2008; Anthony, 1975; Mausz and
510 Chen, 2019). Methylamines can be metabolized by aerobic methylotrophic bacteria (Taubert
511 et al., 2017; Chistoserdova, 2015; Hanson and Hanson, 1996) and by methylotrophic
512 methanogens anaerobically (Chistoserdova, 2015; Thauer, 1998). Based on the data reported

513 in the present study, we suggest that, in addition to methylotrophic methanogenesis, sulfate
514 reduction was involved in MMA consumption in surface sediment of the SBB.

515 Recent literature does implicate anaerobic methylamine oxidation by sulfate reduction.
516 For example, Cadena et al. (2018) performed in vitro incubations with microbial mats collected
517 from a hypersaline environment with various competitive and non-competitive substrates
518 including tri-methylamine. Microbial mats incubated with trimethylamine stimulated
519 considerable methane production; but after 20 days, H₂S began to accumulate and plateaued
520 after 40 days, suggesting that trimethylamine is not exclusively shuttled to methylotrophic
521 methanogenesis. The molecular data reported in Cadena et al. (2018), however, could not
522 identify a particular group of sulfate-reducing bacteria that proliferated by the addition of
523 trimethylamine. Instead, their molecular data suggested potentially other, non-sulfate reducing
524 bacteria, such as those in the family *Flavobacteriaceae* to be responsible for trimethylamine
525 turnover.

526 Zhuang et al., (2019) investigated heterotrophic metabolisms of C1 and C2 low
527 molecular weight compounds in anoxic sediment collected in the Gulf of Mexico. Sediment
528 was incubated with a variety of ¹⁴C radiotracers alone and in combination with molybdate, a
529 known sulfate reducer inhibitor, to elucidate the metabolic turnover of low molecular weight
530 compounds, including ¹⁴C-labeled trimethylamine. Their results showed that although
531 methylamines did stimulate methane production, radiotracer incubations with molybdate and
532 methylamine demonstrated the inhibition of direct oxidation of ¹⁴C-methylamine to ¹⁴C-CO₂,
533 suggesting that methylamines were simultaneously oxidized to inorganic carbon by non-
534 methanogenic microorganisms. This finding further suggests a competition between
535 methanogens and sulfate-reducing bacteria for methylamine; however, the authors could not
536 rule out AOM as a potential contributor to the inorganic carbon pool.

537 Kivenson et al., (2021) discovered dual genetic code expansion in sulfate-reducing
538 bacteria from sediment within a deep-sea industrial waste dumpsite in the San Pedro Basin,

539 California, which potentially allows the metabolization of trimethylamine. The authors
540 expanded their study to revisit metagenomic and metatranscriptomic data collected from the
541 Baltic Sea and in the Columbia River Estuary and found expression of trimethylamine
542 methyltransferase in Deltaproteobacteria. This result suggested that a trimethylamine
543 metabolism does exist in sulfate-reducing bacteria which was enabled by the utilization of
544 genetic code expansion. Furthermore, the results also suggest that trimethylamine could be the
545 subject of competition between sulfate-reducing bacteria and methylotrophic methanogens.

546 Although the evidence of sulfate-reducing bacteria playing a larger role in methylamine
547 utilization is growing, there are other methylotrophic microorganisms in anaerobic settings that
548 could also be responsible for degrading methylamines. De Anda et al. (2021) discovered and
549 classified a new phylum called Brockarchaeota. The study reconstructed archaeal metagenome-
550 assembled genomes from sediment near hydrothermal vent systems in the Guaymas Basin,
551 Gulf of California, Mexico. Their findings showed that some Brockarchaeota are capable of
552 assimilating trimethylamines, by way of the tetrahydrofolate methyl branch of the Wood-
553 Ljungdahl pathway and the reductive glycine pathway, bypassing methane production in
554 anoxic sediment.

555 Farag et al. (2021) found genomic evidence of a novel Asgard Phylum called
556 *Sifarchaeota* in deep marine sediment off the coast of Costa Rica. The study used comparative
557 genomics to show a cluster, *Candidatus* Odinarchaeota within the *Sifarchaeota* Phylum, which
558 contains genes encoding for an incomplete methanogenesis pathway that is coupled to the
559 carbonyl branch of the Wood-Ljungdahl pathway. The results suggest that this cluster could be
560 involved with utilizing methylamines. The *Sifarchaeota* metagenome-assembled genomes
561 results found genes for nitrite reductase and sulfate adenylyltransferase and phosphoadenosine
562 phosphosulfate reductase, indicating *Sifarchaeota* could perform nitrite and sulfate reduction.
563 However, their study did not directly link nitrite and sulfate reduction to the utilization of
564 methylamines by *Sifarchaeota*.

565 Molecular analysis was not performed in the present study; therefore, we are unable to
566 directly link sulfate-reducing or any other heterotrophic bacteria to the direct anaerobic
567 oxidation of methylamine in the SBB. Future work should combine available geochemical and
568 molecular tools to piece together the complexity of metabolisms involved with methylamine
569 turnover and how it may affect the cryptic methane cycle. We note that there appears to be a
570 growing paradigm shift in the understanding of the utilization of non-competitive substrates in
571 anoxic sediment by sulfate-reducing bacteria and methylotrophic methanogens (including
572 other supposedly non-competitive methanogenic substrates like methanol (Sousa et al., 2018;
573 Fischer et al., 2021)). Apparently, methanogens are in fact able to convert these substrates into
574 methane in the presence of their competitors. Which factors provide them this capability should
575 be the subject of future research.

576

577 ***4.4. Implications for cryptic methane cycling in SBB***

578 The SBB is known to have a network of hydrocarbon cold seeps, where methane and
579 other hydrocarbons are released from the lithosphere into the hydro- and atmosphere either
580 perennially or continuously (Hornafius et al., 1999; Leifer et al., 2010; Boles et al., 2004). The
581 migration of methane and other hydrocarbons vertically into the hydrosphere occur along
582 channels that are focused and permeable, such as fault lines and fractures (Moretti, 1998;
583 Smeraglia et al., 2022). Local tectonics and earthquakes could create new fault lines or fractures
584 that reshape or redisperse less permeable sediments, which may open or close migration
585 pathways for hydrocarbons, including methane (Smeraglia et al., 2022). In fact it has been
586 shown that hydrocarbons move much more efficiently through faults when the region in
587 question is seismically active on time scales <100000 yrs (Moretti, 1998). Given the current
588 and historical seismic activity (Probabilities, 1995) and faulting (Boles et al., 2004) within and
589 surrounding the SBB, it is conceivable that hydrocarbon seep patterns and seepage pathways
590 could also shift over time. A potential consequence of this shifting in the SBB is that methane

591 seepage could spontaneously flow through prior non-seep surface sediment. The fate of this
592 methane would then fall on the methanotrophic communities that are part of the cryptic
593 methane cycle. However, it is not well understood how quickly anaerobic methanotrophs could
594 handle this shift due to their extremely slow growth rates (Knittel and Boetius, 2009; Wilfert
595 et al., 2015; Nauhaus et al., 2007; Dale et al., 2008a). After gaining a better understanding of
596 cryptic methane cycling in the SBB presented in this study, a hypothesis worth testing in future
597 studies is whether cryptic methane cycling based on methylotrophic methanogenesis primes
598 surface sediments to respond faster to increases in methane transport through the sediment.

599 **5. Conclusions**

600 In the present study, we set about to find evidence of cryptic methane cycling in the
601 sulfate-reduction zone of sediment along a depth transect in the oxygen-deficient SBB using a
602 variety of biogeochemical analytics. We found that, within the top 10-20 cm, low methane
603 concentrations were present within sulfate-rich sediment and in the presence of active sulfate
604 reduction. The low methane concentrations were attributed to the balance between
605 methylotrophic methanogenesis and subsequent consumption of the produced methane by
606 AOM. Our results therefore provide strong evidence of cryptic methane cycling in the SBB.
607 We conclude that this important, yet overlooked, process maintains low methane
608 concentrations in surface sediments of this OMZ, and future work should consider cryptic
609 methane cycling in other OMZ's to better constrain carbon cycling in these expanding marine
610 environments.

611 Our radiotracer analyses further indicated microbial activity that oxidizes
612 monomethylamine directly to CO₂ thereby bypassing methane production. Based off the sulfate
613 reduction activity and methylamine consumption to CO₂ detected in this study and the
614 metagenomic clues presented in the literature, we hypothesize that sulfate reduction may also
615 be supported by methylamines. Our study highlights the metabolic complexity and versatility
616 of anoxic marine sediment near the sediment-water interface within the SBB. Future work
617 should consider how methylamines are consumed by different groups of bacteria and archaea,
618 how methylamine utility by other anaerobic methylotrophs affects the cryptic methane cycle
619 and evaluate if potential environmental changes affect the cryptic methane cycle activity.

620

621 **Data Availability Statement**

622 Porewater sulfate concentrations and sulfate reduction rates are accessible through the
623 Biological & Chemical Oceanography Data Management Office (BCO-DMO) under the
624 following DOI's:

625 http://dmoserv3.bco-dmo.org/jg/serv/BCO-DMO/BASIN/porewater_geochemistry.html,
626 http://dmoserv3.bco-dmo.org/jg/serv/BCO-DMO/BASIN/sediment_parameters.html,

627 http://dmoserv3.bco-dmo.org/jg/serv/BCO-DMO/BASIN/microbial_activity.html.

628 Sediment methane concentrations and rates and rate constant data of AOM and methanogenesis
629 can be found in the supplementary material Table S2.

630

631

631 **Author Contributions**

632 SK and TT designed the study; SK, JL, DY, DR, DH, QQ, FW, and FJ performed experiments
633 and made measurements; SK, JL, DY, DR, DH, QQ, FW, FJ, DV, and TT analysed the data;
634 SK and TT wrote the manuscript draft with input from all co-authors.

635

636 **Competing Interests**

637 Some authors are members of the editorial board of Biogeoscience. The peer-review process
638 was guided by an independent editor, and the authors have also no other competing interests to
639 declare.

640 **Acknowledgements**

641 We thank the captain and crew of R/V Atlantis, the crew of ROV Jason, the crew of AUV
642 Sentry, and the science party of the research cruise AT42-19 for their technical and logistical
643 support. This work was supported by the National Science Foundation NSF Award NO.: EAR-
644 1852912, OCE-1829981 (to TT), and OCE-1830033 (to DV).

645

646 **References**

647

- 648 Anthony, C.: The biochemistry of methylotrophic micro-organisms, *Science Progress* (1933-),
649 167-206, 1975.
- 650 Arndt, S., Lange, C. B., and Berger, W. H.: Climatically controlled marker layers in Santa
651 Barbara Basin sediments and fine-scale core-to-core correlation, *Limnology and*
652 *Oceanography*, 35, 165-173, 1990.
- 653 Barnes, R. and Goldberg, E.: Methane production and consumption in anoxic marine
654 sediments, *Geology*, 4, 297-300, 1976.
- 655 Beulig, F., Røy, H., McGlynn, S. E., and Jørgensen, B. B.: Cryptic CH₄ cycling in the sulfate-
656 methane transition of marine sediments apparently mediated by ANME-1 archaea,
657 *The ISME journal*, <https://doi.org/10.1038/s41396-41018-40273-z>, 2018.
- 658 Boetius, A., Ravensschlag, K., Schubert, C. J., Rickert, D., Widdel, F., Giesecke, A., Amann, R.,
659 Jørgensen, B. B., Witte, U., and Pfannkuche, O.: A marine microbial consortium
660 apparently mediating anaerobic oxidation of methane, *Nature*, 407, 623-626, 2000.
- 661 Boles, J. R., Eichhubl, P., Garven, G., and Chen, J.: Evolution of a hydrocarbon migration
662 pathway along basin-bounding faults: Evidence from fault cement, *AAPG bulletin*, 88,
663 947-970, 2004.
- 664 Cadena, S., García-Maldonado, J. Q., López-Lozano, N. E., and Cervantes, F. J.: Methanogenic
665 and sulfate-reducing activities in a hypersaline microbial mat and associated
666 microbial diversity, *Microbial ecology*, 75, 930-940, 2018.
- 667 Canfield, D. E. and Kraft, B.: The 'oxygen' in oxygen minimum zones, *Environmental*
668 *Microbiology*, 24, 5332-5344, 2022.
- 669 Capone, D. G., Bronk, D. A., Mulholland, M. R., and Carpenter, E. J.: Nitrogen in the marine
670 environment, Elsevier 2008.
- 671 Chistoserdova, L.: Methylotrophs in natural habitats: current insights through
672 metagenomics, *Applied microbiology and biotechnology*, 99, 5763-5779, 2015.
- 673 Conrad, R.: Contribution of hydrogen to methane production and control of hydrogen
674 concentrations in methanogenic soils and sediments, *FEMS microbiology Ecology*,
675 28, 193-202, 1999.
- 676 Conrad, R.: Importance of hydrogenotrophic, acetoclastic and methylotrophic
677 methanogenesis for methane production in terrestrial, aquatic and other anoxic
678 environments: a mini review, *Pedosphere*, 30, 25-39, 2020.
- 679 Dale, A. W., Van Cappellen, P., Aguilera, D., and Regnier, P.: Methane efflux from marine
680 sediments in passive and active margins: Estimations from bioenergetic reaction-
681 transport simulations, *Earth and Planetary Science Letters*, 265, 329-344, 2008a.

682 Dale, A. W., Regnier, P., Knab, N. J., Jørgensen, B. B., and Van Cappellen, P.: Anaerobic
683 oxidation of methane (AOM) in marine sediments from the Skagerrak (Denmark): II.
684 Reaction-transport modeling, *Geochim. Cosmochim. Acta*, 72, 2880-2894, 2008b.

685 Dale, A. W., Sommer, S., Lomnitz, U., Montes, I., Treude, T., Liebetrau, V., Gier, J., Hensen,
686 C., Dengler, M., Stolpovsky, K., Bryant, L. D., and Wallmann, K.: Organic carbon
687 production, mineralisation and preservation on the Peruvian margin, *Biogeosciences*,
688 12, 1537-1559, 2015.

689 De Anda, V., Chen, L.-X., Dombrowski, N., Hua, Z.-S., Jiang, H.-C., Banfield, J. F., Li, W.-J., and
690 Baker, B. J.: Brockarchaeota, a novel archaeal phylum with unique and versatile
691 carbon cycling pathways, *Nature communications*, 12, 1-12, 2021.

692 Farag, I. F., Zhao, R., and Biddle, J. F.: "Sifarchaeota," a Novel Asgard Phylum from Costa
693 Rican Sediment Capable of Polysaccharide Degradation and Anaerobic
694 Methylootrophy, *Applied and environmental microbiology*, 87, e02584-02520, 2021.

695 Ferdelman, T. G., Lee, C., Pantoja, S., Harder, J., Bebout, B. M., and Fossing, H.: Sulfate
696 reduction and methanogenesis in a Thioploca-dominated sediment off the coast of
697 Chile, *Geochimica et Cosmochimica Acta*, 61, 3065-3079, 1997.

698 Fernandes, S., Mandal, S., Sivan, K., Peketi, A., and Mazumdar, A.: Biogeochemistry of
699 Marine Oxygen Minimum Zones with Special Emphasis on the Northern Indian
700 Ocean, *Systems Biogeochemistry of Major Marine Biomes*, 1-25, 2022.

701 Fischer, P. Q., Sánchez-Andrea, I., Stams, A. J., Villanueva, L., and Sousa, D. Z.: Anaerobic
702 microbial methanol conversion in marine sediments, *Environmental microbiology*,
703 23, 1348-1362, 2021.

704 Gibb, S. W., Mantoura, R. F. C., Liss, P. S., and Barlow, R. G.: Distributions and
705 biogeochemistries of methylamines and ammonium in the Arabian Sea, *Deep Sea
706 Research Part II: Topical Studies in Oceanography*, 46, 593-615, 1999.

707 Hanson, R. S. and Hanson, T. E.: Methanotrophic bacteria, *Microbiol. Rev.*, 60, 439-471,
708 1996.

709 Helly, J. J. and Levin, L. A.: Global distribution of naturally occurring marine hypoxia on
710 continental margins, *Deep Sea Research Part I: Oceanographic Research Papers*, 51,
711 1159-1168, 2004.

712 Hinrichs, K.-U. and Boetius, A.: The anaerobic oxidation of methane: new insights in
713 microbial ecology and biogeochemistry, in: *Ocean Margin Systems*, edited by: Wefer,
714 G., Billett, D., Hebbeln, D., Jørgensen, B. B., Schlüter, M., and Van Weering, T.,
715 Springer-Verlag, Berlin, 457-477, 2002.

716 Hoehler, T. M., Alperin, M. J., Albert, D. B., and Martens, C. S.: Apparent minimum free
717 energy requirements for methanogenic Archaea and sulfate-reducing bacteria in an
718 anoxic marine sediment, *FEMS Microbiol. Ecol.*, 38, 33-41, 2001.

719 Hornafius, J. S., Quigley, D., and Luyendyk, B. P.: The world's most spectacular marine
720 hydrocarbon seeps (Coal Oil Point, Santa Barbara Channel, California): Quantification
721 of emissions, *Journal of Geophysical Research: Oceans*, 104, 20703-20711, 1999.

722 Joye, S. B., Boetius, A., Orcutt, B. N., Montoya, J. P., Schulz, H. N., Erickson, M. J., and Logo,
723 S. K.: The anaerobic oxidation of methane and sulfate reduction in sediments from
724 Gulf of Mexico cold seeps, *Chem. Geol.*, 205, 219-238, 2004.

725 Jørgensen, B. B.: A comparison of methods for the quantification of bacterial sulphate
726 reduction in coastal marine sediments: I. Measurements with radiotracer
727 techniques, *Geomicrobiol. J.*, 1, 11-27, 1978.

728 Jørgensen, B. B.: Bacteria and marine biogeochemistry, in: *Marine biogeochemistry*, edited
729 by: Schulz, H. D., and Zabel, M., Springer Verlag, Berlin, 173-201, 2000.

730 Kallmeyer, J., Ferdelman, T. G., Weber, A., Fossing, H., and Jørgensen, B. B.: A cold
731 chromium distillation procedure for radiolabeled sulfide applied to sulfate reduction
732 measurements, *Limnol. Oceanogr. Methods*, 2, 171-180, 2004.

733 King, G., Klug, M. J., and Lovley, D. R.: Metabolism of acetate, methanol, and methylated
734 amines in intertidal sediments of Lowes Cove, Maine, 45, 1848-1853, 1983.

735 Kivenson, V., Paul, B. G., and Valentine, D. L.: An ecological basis for dual genetic code
736 expansion in marine deltaproteobacteria, *Frontiers in microbiology*, 1545, 2021.

737 Knittel, K. and Boetius, A.: Anaerobic oxidation of methane: progress with an unknown
738 process, *Annu. Rev. Microbiol.*, 63, 311-334, 2009.

739 Kononets, M., Tengberg, A., Nilsson, M., Ekeröth, N., Hylén, A., Robertson, E. K., Van De
740 Velde, S., Bonaglia, S., Rütting, T., and Blomqvist, S.: In situ incubations with the
741 Gothenburg benthic chamber landers: Applications and quality control, *Journal of*
742 *Marine Systems*, 214, 103475, 2021.

743 Krause, S. J. and Treude, T.: Deciphering cryptic methane cycling: Coupling of
744 methylotrophic methanogenesis and anaerobic oxidation of methane in hypersaline
745 coastal wetland sediment, *Geochimica et Cosmochimica Acta*, 302, 160-174, 2021.

746 Kristjansson, J. K., Schönheit, P., and Thauer, R. K.: Different K_s values for hydrogen of
747 methanogenic bacteria and sulfate reducing bacteria: an explanation for the
748 apparent inhibition of methanogenesis by sulfate, *Arch. Microbiol.*, 131, 278-282,
749 1982.

750 Lee, C. and Olson, B. L.: Dissolved, exchangeable and bound aliphatic amines in marine
751 sediments: initial results, *Organic Geochemistry*, 6, 259-263, 1984.

752 Leifer, I., Kamerling, M. J., Luyendyk, B. P., and Wilson, D. S.: Geologic control of natural
753 marine hydrocarbon seep emissions, Coal Oil Point seep field, California, *Geo-Marine*
754 *Letters*, 30, 331-338, 2010.

755 Levin, L.: Oxygen minimum zone benthos: Adaptation and community response to hypoxia,
756 *Oceanogr. Mar. Biol. Ann. Rev.*, 41, 1-45, 2003.

757 Levin, L. A. E., W., Gooday, A. J., Jorissen, F., Middelburg, J. J., Naqvi, S. W. A., Neira, C., and
758 Rabalais, N. N. Z., J.: Effects of natural and human-induced hypoxia on coastal
759 benthos, *Biogeosciences*, 6, 2063–2098, 2009.

760 Lovley, D. R. and Klug, M. J.: Model for the distribution of sulfate reduction and
761 methanogenesis in freshwater sediments, *Geochim. Cosmochim. Acta*, 50, 11-18,
762 1986.

763 Lyu, Z., Shao, N., Akinyemi, T., and Whitman, W. B.: Methanogenesis, *Current Biology*, 28,
764 R727-R732, 2018.

765 Maltby, J., Sommer, S., Dale, A. W., and Treude, T.: Microbial methanogenesis in the sulfate-
766 reducing zone of surface sediments traversing the Peruvian margin, *Biogeosciences*,
767 13, 283–299, 2016.

768 Maltby, J., Steinle, L., Löscher, C. R., Bange, H. W., Fischer, M. A., Schmidt, M., and Treude,
769 T.: Microbial methanogenesis in the sulfate-reducing zone of sediments in the
770 Eckernförde Bay, SW Baltic Sea, *Biogeosciences*, 15, 137– 157, 2018.

771 Mausz, M. A. and Chen, Y.: Microbiology and ecology of methylated amine metabolism in
772 marine ecosystems, *Current Issues in Molecular Biology*, 33, 133-148, 2019.

773 Michaelis, W., Seifert, R., Nauhaus, K., Treude, T., Thiel, V., Blumenberg, M., Knittel, K.,
774 Gieseke, A., Peterknecht, K., Pape, T., Boetius, A., Aman, A., Jørgensen, B. B., Widdel,
775 F., Peckmann, J., Pimenov, N. V., and Gulin, M.: Microbial reefs in the Black Sea
776 fueled by anaerobic oxidation of methane, *Science*, 297, 1013-1015, 2002.

777 Middelburg, J. J. and Levin, L. A.: Coastal hypoxia and sediment biogeochemistry,
778 *Biogeosciences*, 6, 1273-1293, 2009.

779 Moretti, I.: The role of faults in hydrocarbon migration, *Petroleum Geoscience*, 4, 81-94,
780 1998.

781 Nauhaus, K., Albrecht, M., Elvert, M., Boetius, A., and Widdel, F.: In vitro cell growth of
782 marine archaeal-bacterial consortia during anaerobic oxidation of methane with
783 sulfate, *Environ. Microbiol.*, 9, 187-196, 2007.

784 Oremland, R. S. and Polcin, S.: Methanogenesis and sulfate reduction: competitive and
785 noncompetitive substrates in estuarine sediments, *Appl. Environ. Microbiol.*, 44,
786 1270-1276, 1982.

787 Oremland, R. S. and Taylor, B. F.: Sulfate reduction and methanogenesis in marine
788 sediments, *Geochimica et Cosmochimica Acta*, 42, 209-214, 1978.

789 Oremland, R. S., Marsh, L. M., and Polcin, S.: Methane production and simultaneous
790 sulphate reduction in anoxic, salt marsh sediments, *Nature*, 296, 143-145, 1982.

791 Oren, A.: Formation and breakdown of glycine betaine and trimethylamine in hypersaline
792 environments, *Antonie van Leeuwenhoek*, 58, 291-298, 1990.

793 Orphan, V. J., Hinrichs, K.-U., Ussler III, W., Paull, C. K., Tayleur, L. T., Sylva, S. P., Hayes, J. M.,
794 and DeLong, E. F.: Comparative analysis of methane-oxidizing archaea and sulfate-
795 reducing bacteria in anoxic marine sediments, *Appl. Environ. Microbiol.*, 67, 1922-
796 1934, 2001.

797 Paulmier, A. and Ruiz-Pino, D.: Oxygen minimum zones (OMZs) in modern ocean, *Progr.*
798 *Oceanog.*, 80, 113-128, 2009.

799 Probabilities, W. G. o. C. E.: Seismic hazards in southern California: probable earthquakes,
800 1994 to 2024, *Bulletin of the Seismological Society of America*, 85, 379-439, 1995.

801 Qin, Q., Kinnaman, F. S., Gosselin, K. M., Liu, N., Treude, T., and Valentine, D. L.: Seasonality
802 of water column methane oxidation and deoxygenation in a dynamic marine
803 environment, *Geochimica et Cosmochimica Acta*, 336, 219-230, 2022.

804 Ragsdale, S. W. and Pierce, E.: Acetogenesis and the Wood–Ljungdahl pathway of CO₂
805 fixation, *Biochimica et Biophysica Acta (BBA)-Proteins and Proteomics*, 1784, 1873-
806 1898, 2008.

807 Reeburgh, W. S.: Oceanic methane biogeochemistry, *Chem. Rev.*, 107, 486-513, 2007.

808 Reimers, C. E., Ruttenger, K. C., Canfield, D. E., Christiansen, M. B., and Martin, J. B.:
809 Porewater pH and authigenic phases formed in the uppermost sediments of Santa
810 Barbara Basin, *Geochim. Cosmochim. Acta*, 60, 4037-4057, 1996.

811 Rullkötter, J.: Organic matter: the driving force for early diagenesis, in: *Marine*
812 *geochemistry*, Springer, 125-168, 2006.

813 Schimmelmann, A. and Kastner, M.: Evolutionary changes over the last 1000 years of
814 reduced sulfur phases and organic carbon in varved sediments of the Santa Barbara
815 Basin, California, *Geochimica et Cosmochimica Acta*, 57, 67-78, 1993.

816 Sholkovitz, E.: Interstitial water chemistry of the Santa Barbara Basin sediments, *Geochimica*
817 *et Cosmochimica Acta*, 37, 2043-2073, 1973.

818 Smeraglia, L., Fabbi, S., Billi, A., Carminati, E., and Cavinato, G. P.: How hydrocarbons move
819 along faults: Evidence from microstructural observations of hydrocarbon-bearing
820 carbonate fault rocks, *Earth and Planetary Science Letters*, 584, 117454, 2022.

821 Sousa, D. Z., Visser, M., Van Gelder, A. H., Boeren, S., Pieterse, M. M., Pinkse, M. W.,
822 Verhaert, P. D., Vogt, C., Franke, S., and Kümmel, S.: The deep-subsurface sulfate

823 reducer *Desulfotomaculum kuznetsovii* employs two methanol-degrading pathways,
824 *Nature communications*, 9, 1-9, 2018.

825 Soutar, A. and Crill, P. A.: Sedimentation and climatic patterns in the Santa Barbara Basin
826 during the 19th and 20th centuries, *Geological Society of America Bulletin*, 88, 1161-
827 1172, 1977.

828 Stephenson, M. and Stickland, L. H.: CCVII. Hydrogenase. III. The bacterial formation of
829 methane by the reduction of one-carbon compounds by molecular hydrogen,
830 *Biochem. J.*, 27, 1517–1527, 1933.

831 Taubert, M., Grob, C., Howat, A. M., Burns, O. J., Pratscher, J., Jehmlich, N., von Bergen, M.,
832 Richnow, H. H., Chen, Y., and Murrell, J. C.: Methylamine as a nitrogen source for
833 microorganisms from a coastal marine environment, *Environmental microbiology*,
834 19, 2246-2257, 2017.

835 Thauer, R. K.: Biochemistry of methanogenesis: a tribute to Marjory Stephenson,
836 *Microbiology*, 144, 2377-2406, 1998.

837 Treude, T.: Biogeochemical reactions in marine sediments underlying anoxic water bodies,
838 in: *Anoxia: Paleontological Strategies and Evidence for Eukaryote Survival*, edited by:
839 Altenbach, A., Bernhard, J., and Seckbach, J., *Cellular Origins, Life in Extreme Habitats*
840 *and Astrobiology (COLE) Book Series*, Springer, Dordrecht, 18-38, 2011.

841 Treude, T., Krüger, M., Boetius, A., and Jørgensen, B. B.: Environmental control on anaerobic
842 oxidation of methane in the gassy sediments of Eckernförde Bay (German Baltic),
843 *Limnol. Oceanogr.*, 50, 1771-1786, 2005.

844 Treude, T., Smith, C. R., Wenzhoefer, F., Carney, E., Bernardino, A. F., Hannides, A. K.,
845 Krueger, M., and Boetius, A.: Biogeochemistry of a deep-sea whale fall: sulfate
846 reduction, sulfide efflux and methanogenesis, *Mar. Ecol. Prog. Ser.*, 382, 1-21, 2009.

847 Wang, X.-c. and Lee, C.: The distribution and adsorption behavior of aliphatic amines in
848 marine and lacustrine sediments, *Geochimica et Cosmochimica Acta*, 54, 2759-2774,
849 1990.

850 Wang, X.-C. and Lee, C.: Adsorption and desorption of aliphatic amines, amino acids and
851 acetate by clay minerals and marine sediments, *Marine Chemistry*, 44, 1-23, 1993.

852 Wang, X.-C. and Lee, C.: Sources and distribution of aliphatic amines in salt marsh sediment,
853 *Organic Geochemistry*, 22, 1005-1021, 1994.

854 Wehrmann, L. M., Risgaard-Petersen, N., Schrum, H. N., Walsh, E. A., Huh, Y., Ikehara, M.,
855 Pierre, C., D'Hondt, S., Ferdelman, T. G., and Ravelo, A. C.: Coupled organic and
856 inorganic carbon cycling in the deep seafloor sediment of the northeastern
857 Bering Sea Slope (IODP Exp. 323), *Chemical Geology*, 284, 251-261, 2011.

858 Wilfert, P., Krause, S., Liebetrau, V., Schönfeld, J., Haeckel, M., Linke, P., and Treude, T.:
859 Response of anaerobic methanotrophs and benthic foraminifera to 20 years of
860 methane emission from a gas blowout in the North Sea, *Marine and Petroleum*
861 *Geology*, 68, 731-742, 2015.

862 Winfrey, M. R. and Ward, D. M.: Substrates for sulfate reduction and methane production
863 in intertidal sediments, *Appl. Environm. Microbiol*, 45, 193-199, 1983.

864 Wright, J. J., Konwar, K. M., and Hallam, S. J.: Microbial ecology of expanding oxygen
865 minimum zones, *Nature Reviews Microbiology*, 10, 381-394, 2012.

866 Wyrski, K.: The oxygen minima in relation to ocean circulation, *Deep Sea Research and*
867 *Oceanographic Abstracts*, 11-23,

868 Xiao, K., Beulig, F., Kjeldsen, K., Jorgensen, B., and Risgaard-Petersen, N.: Concurrent
869 Methane Production and Oxidation in Surface Sediment from Aarhus Bay, Denmark,
870 *Frontiers in Microbiology*, 8, 10.3389/fmicb.2017.01198, 2017.

871 Xiao, K., Beulig, F., Roy, H., Jorgensen, B., and Risgaard-Petersen, N.: Methylophilic
872 methanogenesis fuels cryptic methane cycling in marine surface sediment,
873 *Limnology and Oceanography*, 63, 1519-1527, 10.1002/lno.10788, 2018.

874 Xiao, K.-Q., Moore, O. W., Babakhani, P., Curti, L., and Peacock, C. L.: Mineralogical control
875 on methylophilic methanogenesis and implications for cryptic methane cycling in
876 marine surface sediment, *Nature Communications*, 13, 1-9, 2022.

877 Zhuang, G.-C., Montgomery, A., and Joye, S. B.: Heterotrophic metabolism of C1 and C2 low
878 molecular weight compounds in northern Gulf of Mexico sediments: Controlling
879 factors and implications for organic carbon degradation, *Geochimica et*
880 *Cosmochimica Acta*, 247, 243-260, 2019.

881 Zhuang, G.-C., Elling, F. J., Nigro, L. M., Samarkin, V., Joye, S. B., Teske, A., and Hinrichs, K.-
882 U.: Multiple evidence for methylophilic methanogenesis as the dominant
883 methanogenic pathway in hypersaline sediments from the Orca Basin, Gulf of
884 Mexico, *Geochim. Cosmochim. Acta*, 187, 1-20, 2016.

885 Zhuang, G.-C., Lin, Y.-S., Bowles, M. W., Heuer, V. B., Lever, M. A., Elvert, M., and Hinrichs,
886 K.-U.: Distribution and isotopic composition of trimethylamine, dimethylsulfide and
887 dimethylsulfoniopropionate in marine sediments, *Mar. Chem.*, 196, 35-46, 2017.

888 Zhuang, G.-C., Heuer, V. B., Lazar, C. S., Goldhammer, T., Wendt, J., Samarkin, V. A., Elvert,
889 M., Teske, A. P., Joye, S. B., and Hinrichs, K.-U.: Relative importance of
890 methylophilic methanogenesis in sediments of the Western Mediterranean Sea,
891 *Geochim. Cosmochim. Acta*, 224, 2018.

892

893